# Separating Genetic And Hemodynamic Defects in Neuropilin-1 Knockout Embryos

Short Title: Genetic and Flow Defects in *nrp-1*$^{-/-}$ Embryos

E. A. V. Jones[1,2], L. Yuan[3], C. Breant[1,2], R. J. Watts[4], A. Eichmann[1,2]

[1] INSERM U833, F-75005, Paris, France.

[2] Collège de France, 11 Place Marcelin Berthelot, 75005 Paris, France.

[3] School of Life Science, Xiamen University 361005 Xiamen, Fujian, China.

[4]Department of Tumor Biology and Angiogenesis, Genentech, Inc., 1 DNA Way, South San Francisco, CA 94080, USA.

Key Words: Neuropilin-1, VEGF, Hemodynamics, Endothelial Cell Migration, Arterial-Venous Differentiation

Corresponding Author:

Elizabeth Jones

Department of Chemical Engineering, McGill University

Rm 4230 Wong Building, 3610 University St

Montreal, Qc, H3A 2B2, Canada

Tel: 514-398-4275

Fax: 514-398-6678

Email: liz.jones@mcgill.ca

## Summary

Targeted inactivation of genes involved in murine cardiovascular development frequently leads to abnormalities in blood flow. Since blood fluid dynamics play a crucial role in shaping vessel morphology, the presence of flow defects generally prohibits the precise assignment of the role of the mutated gene product in the vasculature. In this study, we show how to distinguish between genetic defects caused by targeted inactivation of the Neuropilin-1 (Nrp-1) receptor, and hemodynamic defects occurring in homozygous knockout embryos. Our analysis of a *nrp-1* null allele bred onto a C57BL/6 background shows that vessel remodeling defects occur concomitantly with the onset of blood flow and cause death of homozygous mutants at E10.5. Using mouse embryo culture, we establish that hemodynamic defects are already present at E8.5 and continuous circulation is never established in homozygous mutants. The geometry of yolk sac blood vessels is altered and remodeling into yolk sac arteries and veins does not occur. To separate flow-induced deficiencies from those caused by the *nrp-1* mutation, we arrested blood flow in cultured wild-type and mutant embryos and followed their vascular development. We find that loss of Nrp-1 function rather than flow induces the altered geometry of the capillary plexus. Endothelial cell migration, but not replication is altered in *nrp-1* mutants. Gene expression analysis of endothelial cells isolated from freshly dissected wild-type and mutants and after culture in no-flow conditions showed down-regulation of the arterial marker genes *connexin-40* and *ephrinB2* related to the loss of *nrp-1* function. This method allows genetic defects caused by loss-of-function of a gene important for cardiovascular development to be isolated even in the presence of hemodynamic defects.

# Introduction

The cardiovascular system is one of the few organ systems that must be functional as it develops. In mice, the embryonic heart forms as a linear tube at embryonic day 8 (E8.0) that must beat and supply blood flow before it has undergone looping, trabeculation or compartmentalization. The early blood vessels form as a capillary plexus in an extraembryonic membrane called the yolk sac. Prior to the onset of heart-beat, this plexus is devoid of visible arteries or veins and the vessels lack peripheral cell coverage. When blood first flows through the capillary plexus, the network is rapidly remodeled into a functional circulatory system composed of arteries, veins and capillaries. Structure and function develop in a coordinated manner and proper blood flow is required for normal cardiovascular development (Chapman, 1918; le Noble et al., 2004; Lucitti et al., 2007). If blood flow is stopped or is sufficiently abnormal, the blood vessels remain as a capillary plexus and do not undergo subsequent aspects of cardiovascular development. Therefore the role of signaling molecules in the developing cardiovascular system is often obscured by the varied inputs of an organ system that has already begun to function.

In many cases, null mutations for genes required for proper vascular development also perturb proper blood flow. Genes that are expressed in the endothelium are most often also expressed in the endocardial lining of the heart, which could affect function. Irregularities in vascular geometry, such as occlusions or shunts, can also cause abnormal flow (Jones et al., 2004). Therefore, if a gene is important enough to visibly perturb cardiovascular structures, it will often perturb cardiovascular function as well. Over 50 genes have been published that cause a failure of yolk sac remodeling (personal communication with Mary Dickinson). Though improper blood flow can cause this phenotype, early circulatory function has been investigated in only a minority of these embryos. Vascular abnormalities present in the N-cadherin null mouse can be rescued by

restoring normal blood flow using cardiac-specific expression of either N- or E-cadherin (Luo et al., 2001), indicating that the observed vascular abnormalities are secondary to the abnormal blood flow. Abnormal or absent blood flow has been shown to cause failure to remodel in embryos (Lucitti et al., 2007), more cuboidal endothelial cell shape (May et al., 2004), vessel regression (Clark, 1918; Meeson et al., 1996; Thoma, 1893), abnormalities in peripheral cell recruitment (Grazioli et al., 2006) and changes in vessel diameter (Thoma, 1893). Proper vascular development requires a complex interaction of both genetic and physical signals, where one cannot develop normally without the other. It is therefore essential to separate when these events occur because of the mutation of interest and when they are induced by abnormal blood flow.

The Neuropilin-1 (Nrp-1) receptor was originally identified as a receptor for the axon guidance molecule Semaphorin3A and is implicated in the development of the nervous system (He and Tessier-Lavigne, 1997; Kolodkin et al., 1997). Nrp-1 is also an isoform-specific receptor for $VEGF_{165}$ (Soker et al., 1998) and plays an important role in the cardiovascular system, as deletion of the *nrp-1* gene leads to embryonic lethality due to cardiovascular malformations. Lethality occurs between E10.5 and E13.5, depending on the genetic background (Kitsukawa et al., 1997). On a CD-1 background, embryos lacking *nrp-1* exhibit defects in the formation of the heart outflow tract and aortic arches (Kawasaki et al., 1999). In addition, they exhibit abnormal vascular network formation in the yolk sac (Kawasaki et al., 1999) and abnormal sprouting of hindbrain vessels (Gerhardt et al., 2004). Furthermore, in endothelial-specific *nrp-1* knockouts, certain arterial markers are missing from arterioles and arteries (Mukouyama et al., 2005). The presence of both cardiac and vascular defects indicated that *nrp-1* null embryos could present abnormal blood flow patterns and that aspects of their phenotype could be induced by improper

flow rather than by loss of function of the receptor. We therefore decided to examine flow patterns in relation to vascular defects in these embryos.

We investigate here the cardiovascular phenotype of a *nrp-1* mutant allele (Gu et al., 2003) bred on a C57BL/6 background. *Nrp-1*$^{-/-}$ embryos die at E10.5 with severe vascular abnormalities that are accompanied by abnormal flow patterns. In order to separate flow-induced defects from defects induced by the *nrp-1* mutation, we compared wild-type and mutant embryos in the absence of flow. We find that the yolk sac vascular defects are not related to the flow defect but due to loss of Nrp-1 function. Function-blocking anti-Nrp-1 antibodies (Pan et al., 2007a) injected into wild-type embryos can reproduce the yolk sac vessel defects observed in *nrp-1* mutants in a normal flow environment. By identifying an aspect of the mutant phenotype that is not dependent on flow, we are then able to investigate the genetic causes of this defect. We find that *nrp-1*$^{-/-}$ endothelial cells exhibit normal replication, but altered migration and defective arterial differentiation.

# Materials And Methods

## Mice

*Nrp-1* mutant mice on a C57BL/6 background were generated as described (Gu et al., 2003). Briefly, a conditional targeted allele contained two *loxP* sites flanking exon 2 of the *nrp-1* gene was created. *Npn-1* null mice were obtained by crossing mice harboring this conditional allele with mice expressing Cre recombinase in the germline. The colony was maintained by breeding heterozygous male mice with wild-type C57BL/6 (Charles River Laboratories). Genotyping was performed using Ready-to-go PCR beads (Amersham Pharmacia Biotech, No. 27955801) with

forward primer GCC AAT CAA AGT CCT GGA AGA CAG and reverse primer CTG CAG ATC ATG TAT ACT GGT GAC.

## Immunohistochemistry and In Situ Hybridization

For whole mount stainings, embryos were fixed in Dent's fixation (4 parts MeOH: 1 part DMSO) overnight at 4°C. Embryos were progressively rehydrated and blocked twice for one hour in TNB (Roche No. 11096176001). Embryos were incubated overnight at 4°C with primary antibodies (1:100) in TNB (biotinylated α-PECAM-1, BD Bioscience No. 553371; rabbit α-human Collagen IV, Serotec No. 2150-0140; phospho-histone 3, Abcam No. ab5176-100). Embryos were washed, re-blocked and incubated overnight with fluorescent streptavidin or fluorescent secondary antibodies (1:400) at 4°C.

For sections, embryos were dissected and fixed in 4% PFA overnight at 4°C. Embryos were washed in 70% ethanol, stained with eosin, dehydrated and embedded in paraffin. Immunohistochemistry was performed using the Tyramide Signal Amplification system (TSA™, NEN™ Life Science Products, Boston, MA).

In situ hybridization has been described previously (Moyon et al., 2001a) with probes for *dll4* (Suchting et al., 2007), *nrp-1* (Yuan et al., 2002), *efnb2* (Moyon et al., 2001b) and *cx40* (Mukouyama et al., 2005).

## Quantitation of Vascular Phenotype

After PECAM-1 stainings, yolk sacs were mounted and imaged on a fluorescent microscope (magnification 20x). Using ImageJ, images were filtered and converted to binary images. Total vessel area was assessed by counting the number of white vs black pixels in the binary images. Network morphology was quantified using the Biologic Analyzer, a software program developed by Nicolas Elie (Centre de Morphologie Mathematiques-ARMINES, France). This program extracts the skeleton of the vascular network from binary images (Beucher, 1990; Coster and Chermant, 1985) and points where the skeleton lines intersect are counted as branchpoints (Ablameyko and Pridmore, 2000) (Suppl. Fig. 1). Segment length was assessed by dividing the total length of all skeleton lines by the number of intersections. Vessel diameter was assessed indirectly, by measuring the average area of an avascular space (hole) between vessels. Four to five images per yolk sac and a minimum of three yolk sacs per group were analyzed.

## Flow Assessment and Creation of No Flow Embryos

Breeding pairs of mice were mated overnight and the presence of a vaginal plug denoted E0.5. Embryos were collected at E8.5 and cultured as described (Jones et al., 2002) except that roller culture rather than static culture was used. For analysis of flow, embryos were collected at 5 somites and cultured for 6 or 24 hours. The yolk sac was observed under white light (10x magnification), focusing especially on the outlet of the dorsal aorta where the fastest and most visible flow is located. Embryos were time-lapsed by placing them on a heated stage after culture and images were taken with white light at a rate of approximately 2 Hz.

To create no flow embryos, 3-4 somite stage embryos were held with No. 5 watchmaker forceps and the yolk sac and inlets to the heart were snipped on both sides of the heart using No. 55

watchmaker forceps. The embryos were then cultured for 24 hours. Most embryos recovered from the injury and had normally inflated yolk sacs (not shown) though the inlet to the heart was deformed and embryos never turned. 1-2 embryos per litter had deflated yolk sacs or still had blood circulation and were discarded.

## Embryo Injections And Migration Assay

Injections were performed using a pulled quartz needle filled with either 70,000 MW Texas Red dextran (Molecular Probes, No. D-1828) for angiograms, or protein solutions (Nrp-1 blocking antibodies, Pan et al., 2007a, all others from R&D systems) for Nrp-1 blocking experiments. For protein solutions, a small quantity of 70,000 MW Texas Red dextran was added to visualize injection. A picospritzer II (General Valve Corp.) was used to inject, the volume of the injections was set by varying the pressure until the desired amount of dye was expunged. The needle was inserted into the heart of the embryos (10 somites for angiograms, 4 somites for protein solutions), through the yolk sac. Long thin quartz needles were used to prevent damage to the yolk sac. Several pulses of solution were injected into the beating heart and dye could be visualized during injection entering the yolk sac and filling the vessels. This ensured accurate and specific dosing to only the cardiovascular system. Approximate dosing of protein solutions was calculated using an order of magnitude estimation. An embryo's dimensions are about 1mm x 100 μm x 100 μm at this stage and the density of an embryo is approximately equal to that of water. With approximately 10 nL of protein solution injected (4.4 mg/mL and 7.6 mg/mL for α-Nrp-1A and α-Nrp-1B respectively), the dose is an order of magnitude of $10^3$-$10^4$ mg of protein/kg of embryo.

In the case of the migration assay, CM-DiI (Invitrogen, no. C7001) dye was injected focally onto the yolk sac. Embryos (n=23 wild-type or heterozygotes, 5 *nrp-1*$^{-/-}$) were cultured for 24 hours and then photographed using bright-field and fluorescent light on a Leica fluorescent dissecting microscope. Using photoshop, the distance from the center of the injection site to the most distant fluorescent endothelial cell was measured.

### Isolation of Embryonic Endothelial Cells and Quantitative RT-PCR

Embryos were collected at E9.5 or after 24 hours of culture starting at E8.5. Two to three embryos that appeared to be of the same genotype were pooled and digested with collagenase for 40 minutes. Endothelial cells were then separated using Dynabeads (Invitrogen No. 110-35) coated with PECAM-1 antibody (BD Bioscience No. 553369), non-endothelial cells were collected for genotyping. Endothelial cell RNA was extracted using an RNeasy micro kit (Qiagen No. 74004). Retrotranscription was performed using MMLV reverse transcriptase and Oligo dT primers. SYBR green PCR mix (Qiagen No. 204145) and a Biorad iCycler were used to quantitate gene expression in these samples. All primers were QuantiTect Primer Assays (Qiagen). A total of 6 sets of 2-3 embryos with the correct genotype was used quantitate gene expression in each group.

## Results

### Cardiovascular Phenotype of the *nrp-1*$^{-/-}$ Embryos

Neuropilin-1 (*nrp-1*) knock-out mice were generated by crossing mice harboring a conditional *nrp-1* allele with mice expressing Cre recombinase in germ cells, as described (Gu et al., 2003).

Chimeras were backcrossed on a pure C57BL/6 background for > 7 generations. We examined the cardiovascular phenotype between E8.0 (4-6 somites) and E11.5.

In wild-type embryos, the earliest vessels form in the yolk sac, an extra-embryonic tissue that surrounds the developing embryo. This *de novo* vessel formation occurs between E8.0 and E8.5 and is known as vasculogenesis. As these early vessels connect to the embryonic heart and the heart begins to beat, the yolk sac vasculature is remodeled into a more hierarchical structure composed of arteries, capillaries and veins that can be visualized at E9.5 in freshly dissected embryos and by staining with the pan-endothelial marker PECAM-1 (Fig. 1A, B). *Nrp-1* null embryos fail to undergo vascular remodeling and exhibit poorly branched, enlarged vessels throughout the yolk sac at E9.5 (Fig. 1E, F). The caliber of yolk sac vessels in *nrp-1*$^{-/-}$ embryos is similar to that of large arteries of the yolk sac in the wild-type embryos (Fig. 1B, F). As well, large avascular spaces are observed between the mutant vessels (Fig. 1E, F).

*De novo* formation of blood vessels in *nrp-1* null embryos appeared identical to wild-type until E8.5 (data not shown), suggesting a possible requirement of *nrp-1* during the process of vessel remodeling but not vessel formation. To determine when the mutant phenotype became apparent, we injected fluorescently tagged dextran into the heart of normal (Fig. 1C) and mutant embryos (Fig. 1G) at 10 somites (E8.75), just after the normal onset of blood flow. The dextran highlights the vasculature of the heart, yolk sac and dorsal aortae in both wild-type and knockout embryos, indicating that lumenized vessels are present in *nrp-1*$^{-/-}$ embryos. However, the large dilated vessels and avascular spaces were already apparent in the mutant yolk sacs at this stage, indicating that the phenotype appears concomitantly with the onset of blood flow.

To quantitate the difference in the vascular phenotypes, we performed morphometric analysis (Suppl. Fig. 1) and measured total vessel coverage, the number of vessel branch points, segment length and avascular spaces between capillaries on PECAM stained yolk sacs of wild-type and mutants (Fig. 1D, H). Before the onset of flow (E8.0, 4-6 somites), there was no statistically significant difference in overall vessel coverage, number of branchpoints or segment length between embryos of different genotypes (Fig. 1I-K). Overall vessel coverage remained similar between wild type and *nrp-1* mutants at subsequent developmental stages (data not shown). However, the number of vessel branchpoints decreased in the *nrp-1* mutant yolk sacs just after the onset of blood flow at 7-10 somites (E8.5) and at 20-25 somites (E9.5) (Fig. 1I). If the total vessel area is constant, and the number of vessel branchpoints is reduced, one expects that the length of individual vessel segments increases, which is what we observed in the *nrp-1* mutant compared to wild-type (Fig 1J). The average size of avascular areas (holes) separating capillaries increased in *nrp-1*$^{-/-}$ mutants compared to wild-type both at 7-10 somites and at 20-25 somites (Fig. 1K). With constant vessel area and increased space between vessels, it follows that the individual segments must be thicker. Taken together, this quantification revealed that *nrp-1* null yolk sac vessels show normal overall vessel coverage, but altered vascular geometry, with less branched, thicker vessels separated by large avascular spaces and that these defects appear concomitantly with the onset of blood flow.

Examination of the embryo proper between E8.5 and E9.5 showed that somite addition in *nrp-1*$^{-/-}$ embryos occurred at normal rate until E9.5 (23 to 25 somites), but ceased afterwards. A developmental delay of *nrp-1*$^{-/-}$ compared to wild-type or heterozygous littermates became apparent at E9.5. Live knockout embryos could be recovered until E10.5, but were severely growth retarded at this stage (data not shown). Taken together, we observe that *nrp-1*$^{-/-}$ embryos on the C57BL/6 background die at E10.5, consistent with previous reports of a different *nrp-1*

mutant allele bred on this background (Kitsukawa et al., 1997), and exhibit vessel remodeling defects that appear concomitant with the onset of blood flow.

## *Nrp-1*$^{-/-}$ Embryos Exhibit Abnormal Blood Flow

Since proper blood flow is required for remodeling to occur (le Noble et al., 2004; Lucitti et al., 2007), we next investigated whether normal blood flow was present in *nrp-1*$^{-/-}$ embryos. In wild type embryos, the heart starts beating at the 3-somite-stage, initiates a period of plasma flow through the primitive vascular plexus from 3 somites until 5-6 somites, which is followed by the gradual entry of erythroblasts into circulation. Continuous circulation, where vessels are consistently filled with flowing erythroblasts, is established by approximately 8 somites (Lucitti et al., 2007). We investigated whether erythroblasts circulated in *nrp-1*$^{-/-}$ mutants by placing embryos at E8.5 (5-7 somites) into culture for 6 or 24 hours, as previously described (Jones et al., 2004). The embryos were removed from culture and observed under white light for circulating erythroblasts (Table I). Using this method, we saw erythroblasts circulating in 100% of E8.5 wild-type embryos (n=12, Suppl. Movie1) and 100% of E9.5 wild-type embryos (n=13). In contrast, normal circulation was not observed at either stage in embryos lacking *nrp-1*. In E8.5 mutant embryos, erythroblasts could only be seen oscillating in place (Table I, Suppl. Movie 2) and continuous movement of erythroblasts through the early vascular plexus was never observed. By E9.5, no erythroblast motion was observed in the mutant embryos (n=4) and circulation had completely arrested. Thus, *nrp-1* homozygous mutants can initiate heart contraction and plasma flow (Fig. 1G), but fail to initiate erythroblast circulation.

To investigate possible causes of the defective blood flow, we sectioned and stained wild-type and mutant embryos at E8.5 and E9.5 (Fig. 2). *Nrp-1* expression in arteries of the E8.5 (10

somite stage) embryo and yolk sac vessels (Fig. 2A), detected by *in situ* hybridization, provided a possible causative explanation for the vascular remodeling defect. In addition, *nrp-1* stained the atrial compartment of the heart (Fig. 2A). By RT-PCR, we could detect *nrp-1* expression in the heart as early as 4 somites (n = 4), and this expression was sustained at 7 somites (n=4) and 10 somites (n=4).

Lack of cardiac *nrp-1* expression could cause the observed blood flow defects, as oscillatory flow has previously been seen in embryos that specifically lack the atrial component of heart contractions (Lucitti et al., 2007). The heart of *nrp-1* null embryos underwent proper looping at E8.5, however the pericardial sac of the mutant embryos was consistently enlarged by E10.5 (n=7) and no trabeculation was observed from E9.5 onwards. At E8.5, the endocardial lining stained positively for PECAM-1 and was present in both wild-type and mutant embryos (data not shown). The size of the heart also appeared to be normal. Therefore, the heart appeared morphologically normal at 10 somites when flow problems could already be observed. To determine if heart function was normal in the *nrp-1* null embryos, we placed embryos at the 6 somite stage into culture for 6 hours and observed the form of the heart contraction. Heart contractions initiate at the base of the heart and move anteriorly in both wild-type and *nrp-1* knockout embryos (n=8 for wt and n=3 for mutant). Heart rate also did not differ significantly between wild-type and mutant (51± 4.5 bpm and 40± 5.7 bpm, respectively, Supplemental Movies 1, 2). We therefore conclude that heart function is also grossly normal in the mutant embryos, although more subtle defects could not be detected with this method.

Since cardiac function appeared grossly normal, we next looked at whether the vasculature of the embryo proper had formed normally. PECAM-1 staining at E8.5 showed that both dorsal aortae were present in wild type (Fig. 2B) and mutant embryos (Fig. 2D). The diameter of these vessels appeared normal throughout the embryo, but *Nrp-1*$^{-/-}$ vessels were often collapsed, perhaps

impeding blood flow and circulation, although the dextran injections showed that vessels were lumenized at this stage (Fig. 1G). At E9.5, Collagen IV staining on sections from wild-type embryos revealed two dorsal aortae on either side of the neural tube (Fig. 2C). One or both of these vessels, at the level of the heart, were missing in *nrp-1* mutant embryos (Fig. 2E, G, Fig. 4B), though they were generally still present at the caudal end of the embryo. E9.5 *nrp-1* mutant embryos also showed delayed vessel sprouting into the intersomitic regions when compared to wild-type (Fig. 2F,G), though sprouts that progressed far enough interconnected as in wild-type. The cephalic vascular plexus developed in *nrp-1*$^{-/-}$ embryos, although the vessels were thinner and sparser than in normal embryos and did not appear to be lumenized (Fig. 2H,I). Smooth muscle cells, visualized with α-SMA staining, surrounded the major vessels of the embryo in wild-type embryos, but were not present either in the head or trunk region of homozygous mutant embryos (data not shown).

## Separating the Role of Blood Flow From Nrp-1 Function

As the histological and functional analysis of the cardiovascular system in *nrp-1* null embryos did not reveal a major defect in the mutant heart or vessels of the embryo proper, the yolk sac vascular phenotype in *nrp-1*$^{-/-}$ mice could be due to defective flow causing defective vessel remodeling or *vice versa*. We therefore sought to differentiate primary effects caused by lack of *nrp-1* from secondary defects caused by abnormal flow.

We suspected a direct role of Nrp-1 signaling during the formation of yolk sac vessels, because the vascular phenotype in the yolk sac of *nrp-1* null embryos was not the same as published for embryos that completely lack flow, such as the *ncx1*$^{-/-}$ embryos (Wakimoto et al., 2000), or

embryos that exhibit only oscillatory flow, such as the *mlc2a*$^{-/-}$ embryos that we have previously analyzed (Lucitti et al., 2007). We therefore created embryos that completely lacked flow in order to compare the vasculature of wild-type "no flow" embryos with those of *nrp-1* mutants. By placing wild-type and mutant embryos into the same no-flow mode, the comparison of the phenotypes reflects only the role of *nrp-1* and not normal vs. abnormal or absent flow. We created no flow embryos by snipping the inlet to the heart in 4 somite embryos (see Methods), a stage when the heart has started beating but erythroblast circulation has not initiated. These embryos are then cultured for 24 hours using whole embryo roller culture. The presence or absence of flow is evaluated after culture at a stage when circulation of erythroblasts is normally evident. The vasculature is then stained using antibodies to PECAM-1 and the number of vessel branch points, vessel segment length and avascular spaces are quantitated.

In wild-type embryos with normal flow, key aspects of vascular remodeling were apparent after culture, such as changes in branch angle and the formation of large vessels in the yolk sac. These large, regularly branched vessels are separated by capillary regions (Fig. 3A). As observed in freshly dissected embryos (Fig. 1F), cultured *nrp-1* mutants fail to undergo remodeling and to create a hierarchical branching system (Fig. 3A). Though the overall vascular coverage was not affected in *nrp-1* mutants (n= 12 for wild-type, n=10 for mutant, data not shown), the yolk sac vessels showed decreased branching, increased segment length and large spaces separating vessels. The difference in vessel diameter between wild-type and mutant embryos was also apparent in sections (inlays, Figure 3A).

Comparing embryos in the no flow environment, we found that wild-type and knockout embryos did not show the same vascular phenotype (Figure 3A). In wild-type no flow embryos, large

vessels never formed and the entire vasculature remained reminiscent of the capillary regions of the yolk sac with blood flow. Vessel branching was decreased (Fig. 3B), however no change in segment length or in the area of avascular spaces was present compared to embryos experiencing normal flow (Fig 3C, D). Cultured no flow *nrp-1*$^{-/-}$ embryos also showed decreased branching (Fig. 3B), but, in addition showed increased segment length (Fig. 3C) and increased area of avascular spaces (Fig. 3D), similar to the vascular phenotype of *nrp-1*$^{-/-}$ embryos in normal flow conditions and in striking contrast to the phenotype of wild-type no-flow embryos. Thus, all aspects of the *nrp-1*$^{-/-}$ yolk sac vessel phenotype develop in no-flow culture conditions, indicating that the phenotype is due to loss of Nrp-1 function.

## Blocking Nrp-1 Function Reproduces the *nrp-1-/-* Yolk Sac Vessel Phenotype

Having determined that loss of Nrp-1 function, rather than disturbed blood flow, was responsible for the altered vascular geometry in the yolk sac of *nrp-1*$^{-/-}$ embryos, we reasoned that blocking Nrp-1 function in wild-type embryos should reproduce the vascular phenotype observed in *nrp-1* null mutants. We used antibodies that specifically block either Sema3A or VEGF-A binding to Nrp-1 (Pan et al., 2007a). Treated embryos were cultured for 24 hours, PECAM-1 stained (Fig. 4A-D) and yolk sac vessel branching and avascular spaces were quantified (Fig. 4E- G). To optimize protein delivery to the yolk sac, we first compared direct addition of protein to the medium of cultured embryos and intracardiac injection of protein solution, using $VEGF_{120}$, which is expected to increase vessel coverage. We found that intracardiac injection was preferable since $VEGF_{120}$ could not diffuse across the yolk sac when added directly to the medium (data not shown). Injection of $VEGF_{120}$ led to an increase in the vascular coverage (from 74.1% ± 1.1 to 85.9% ± 1.1) such that most of the yolk sac stained positive for PECAM-1 (Fig. 4B). Having

optimized protein delivery, we analyzed the effects of intracardiac injection of Nrp-1 blocking antibodies (Pan et al., 2007a). Anti-Nrp-1A antibody blocks Sema3A binding and anti-Nrp-1B is specific for the VEGF binding domain of Nrp-1, though both prevent receptor dimerization with VEGFR-2. Both antibodies were capable of decreasing vessel branching and increasing segment length (Fig. 4C-F). Anti-Nrp-1A had no effect on the area of avascular regions, but anti-Nrp-1B was able to create large avascular regions similar to those seen in the *nrp-1*$^{-/-}$ embryos (Fig. 4C, D, G). Injection of both antibodies together did not create a synergistic effect on branching, and effects on avascular spaces were similar to the ones seen with anti-Nrp-1B alone (Fig 4G). Attempts at blocking Nrp-1 function by injection of soluble Nrp-1, which should sequester Nrp-1 ligands including $VEGF_{165}$ (Gagnon et al., 2000), had no effect on yolk sac vasculature (Fig. 4E-G). Injection of the Nrp-1 ligand Sema3A, which had previously been shown to compete with $VEGF_{165}$ for Nrp-1 binding (Miao et al., 1999), also had no significant effects (Fig 4E-G), consistent with recent data showing directly that Sema3A and VEGF do not compete for binding to Nrp-1 (Appleton et al., 2007), and that Sema3A mutant mice lack an observable vascular phenotype (Vieira et al., 2007). Though no effects were observed in these injection experiments, it was not possible to assess whether larger quantities of protein could have elicited a response. The embryo and its network of blood vessels are small at this stage and limit how much protein solution can be injected into the embryo without causing injury. However, inhibition of Nrp-1 function with a blocking antibody to the VEGF binding domain in wild-type embryos could clearly reproduce the altered vascular geometry observed in *nrp-1* knockout yolk sacs, confirming that this aspect of the phenotype was due to loss of Nrp-1 function and not to altered blood flow.

## Replication, sprouting, regression and migration in *nrp-1-/-* vessels

Nrp-1 has been implicated in sprouting (Gerhardt et al., 2004), migration (Pan et al., 2007b) and proliferation of endothelial cells (Soker et al., 1998). We therefore investigated how endothelial cell behavior in the yolk sac was different between mutant and wild-type embryos. Endothelial cell replication was assessed at various developmental stages in wild-type and mutant embryo yolk sacs using phospho-histone H3 and PECAM-1 double-staining (Fig. 5A). No significant difference in the number of dividing endothelial cells was observed between the two groups at all stages investigated (n=3-4 embryos per group with five images per embryo). Replication of smooth muscle cells and of total cells in the yolk sac at E9.5 was also similar between *nrp-1* knockouts and wild type (not shown). Taken together with the similar total vessel coverage observed in wild type and knockouts, these results indicate that endothelial replication is unlikely to account for the observed yolk sac vessel defects in *nrp-1* knockouts. The sprouting and regression of vessels was assessed by counting the number of PECAM-1 stained endothelial cells extending into avascular spaces of the yolk sac, such that they formed dead-ended vessels (unconnected extensions). No differences were observed between the different groups and the presence or absence of flow did not affect this measure (Fig. 5B).

Endothelial cell migration was assessed by focal injection of a lipophilic carbocyanine dye (DiI) using a picospritzer into a capillary region of the yolk sac (red arrow, Fig. 5D, E) followed by culture to allow marked cells to migrate. Regions where the fluorescence is continuous from cell to cell indicate endothelial cells migrating away from the site of injections (Fig. 5F, G). In wild-type embryos, marked cells migrate but remain confined within proximity to the injection site (Fig. 5C, D, F, n= 23). *Nrp-1* knockout DiI positive cells migrate along the abnormally formed

yolk sac capillaries and are found at greater distances from the injection area than wild-type cells (Fig. 5C, E, G, n= 5). Quantification of the distance of cell migration confirmed that endothelial cells migrated further away from the injection site in *nrp-1*$^{-/-}$ compared to wild-type yolk sacs (Fig. 5C), indicating that they exhibit abnormal migration.

## Defective Arterial Differentiation in *Nrp-1-/-* Embryos is Not Flow Related

Previous reports have indicated that arterial differentiation is defective in endothelial-specific *nrp-1* knockouts (Mukouyama et al., 2005). Though arterial identity is established before the onset of flow, the expression of arterial markers remains plastic and changes with the flow that endothelial cells are exposed to. If an embryonic artery is ligated to create an environment where the vessels experience venous flow, expression of markers such as ephrinB2 will be downregulated and expression of venous markers will be upregulated (le Noble et al., 2004). Other groups have also shown that endothelial cells change their gene expression depending on the waveform of the flow that they are exposed to (Blackman et al., 2002). We therefore investigated whether changes in arterial-venous gene expression in *nrp-1* mutants were created by the abnormal flow present in these embryos.

We examined the expression pattern of arterial markers Delta-like-4 (*dll4*), Connexin-40 (*cx40*) and Ephrin-B2 (*efnb2*) by *in situ* hybridization in both wild-type and mutant embryos (Fig. 6A-F). At E9.5, *dll4* was expressed in the common atrial chamber of the heart and in the dorsal aorta of wild-type or heterozygous embryos (Fig. 6A). In *nrp-1*$^{-/-}$ embryos (Fig. 6B), we observed expression both in the common atrial chamber and in the dorsal aorta (when present, red arrow denotes missing second dorsal aorta). *Cx40* expression can be seen specifically in the common

atrial chamber and in the dorsal aorta for wild-type embryos (Fig. 6C). This expression is completely lacking in *Nrp-1*$^{-/-}$ embryos (Fig. 6D). *Efnb2* was expressed in the somites, neural tube, the dual dorsal aortae and the vitelline artery of wild-type (Fig. 6E). *Nrp-1*$^{-/-}$ embryos showed normal *efnb2* expression in somites and neural tube, as well as staining in the endothelium of the dorsal aorta, but labeling of the vitelline artery was reduced compared to wild-type or heterozygous littermates (Fig. 6F).

To further explore differences in gene expression between *nrp-1*$^{-/-}$ and wild-type embryos, we used quantitative RT-PCR. Endothelial cells were isolated from 2-3 embryos using Dynabeads coated with antibodies against PECAM-1 (see Methods). From this cell population, RNA was extracted and analyzed. To rule out effects of flow induced gene expression, we also tested endothelial cell gene expression in wild type and mutant embryos that lacked flow. In all, 6 sets of 2 to 3 embryos were analyzed per group. The relative expression levels were measured for 11 cardiovascular genes (Fig. 6G); 4 pan-endothelial, 4 arterial and 3 venous. These were normalized to 3 housekeeping genes, *β-actin*, α-*tubulin* and *gapdh*. Most genes showed no significant difference in expression level between wild-type, *nrp-1*$^{-/-}$, no-flow wild-type and no-flow knockout (*hif1α, vegfr2, ve-cadherin, dll4, nrp-2* and *ephB4*). Expression of v*egf-a* and *unc5b* was altered in endothelial cells of *nrp-1* mutants compared to wild type (Fig. 6G). Stopping flow, however, eliminated the difference between wild-type and mutant indicating that no difference is seen when observed on the same flow background. *CouptfII* levels were unaffected by the *nrp-1* mutation but were decreased in no-flow conditions (Fig. 6G). In contrast to these genes, expression of the arterial markers *efnb2* and *cx40* was specifically down-regulated in *nrp-1* mutants (Fig. 6G), as reported previously in endothelial-specific *nrp-1* knockouts (Mukouyama et al., 2005). The decrease in *efnb2* levels was modest, confirming the *in situ* hybridization results indicating that not all vessels lost *efnb2* expression, while expression of *cx40* was strongly

decreased in *nrp-1* mutants. Down-regulation of *efnb2* and *cx40* was not flow related but specific to loss of *nrp-1,* since the difference was present between no-flow wild type and knockout embryos as well.

# Discussion

## Vessel remodeling and flow defects in *Nrp-1-/-* mutants

In this work, we study the role of Nrp-1 in cardiovascular development. A previous study of *nrp-1*$^{-/-}$ embryos showed that embryonic lethality occurred at E10.5 on a C57BL/6 background, but only at E13.5 on a CD-1 background (Kitsukawa et al., 1997). Cardiovascular defects in *nrp-1* mutants were so far only analyzed in the CD-1 mutants (Kawasaki et al., 1999) and in endothelial-specific conditional mutants, which also die at E13.5 (Gerhardt et al., 2004; Gu et al., 2003; Mukouyama et al., 2005). In agreement with the initial report (Kitsukawa et al., 1997), our extensive analysis of an *nrp-1* mutant allele bred on C57BL/6 showed lethality at E10.5. In fact, these *nrp-1*$^{-/-}$ embryos show arrest of all cardiovascular progress one day after cardiovascular function normally begins. The heart has looped but no trabeculations form. The dorsal aortae form normally at E8.5 but are regressing by E9.5, and smooth muscle cells do not surround large vessels. Yolk sac vessels fail to remodel into arteries and veins, show reduced branching, diameter increase and enlarged avascular spaces. The embryo begins to appear necrotic by E9.5 and is slowly resorbed by E11.5. Analysis of flow patterns showed that normal flow was never observed in *nrp-1* null mutants. As vascular defects appear concomitantly with blood flow defects, they could be secondary to the flow defects or caused by the *nrp-1* mutation.

Though blood flow was aberrant in the *nrp-1*$^{-/-}$ embryos, no major cardiovascular defects were observed in the embryo proper when flow defects first became visible. Heart development and function were normal and all the major vessels of the embryo were present and lumenized at E8.5. More subtle changes in heart function cannot be measured at these young stages and remain a possible cause of flow insufficiencies. However, the defects in the yolk sac vasculature may actually cause the abnormal flow. When the heart begins to contract at 3 somites, a period of plasma flow is initiated (Lucitti et al., 2007). As heart development continues, plasma flow increases and eventually carries erythroblasts into circulation. Enlarged yolk sac vessels would require a larger pump (or stronger heart) than normal to create an equivalent velocity of plasma flow in the vessels given the laws of conservation of mass. If the plasma is not flowing fast enough, then the erythroblasts cannot circulate. *Nrp-1*$^{-/-}$ embryos on a CD-1 background are not resorbed until E13.5 (Kitsukawa et al., 1997), although they show aberrant yolk sac vessel geometry similar to the one described here (Kawasaki et al., 1999). We speculate that the difference in the stage at which the mutant embryos die in these two backgrounds could be due to slightly increased embryo growth rate, heart contractility and blood flow in CD-1 versus C57BL/6 embryos, which would be sufficient to initiate blood flow but still encounter altered vascular geometry and eventually fail to establish proper circulation.

## Separating genetic and flow defects in *Nrp-1*$^{-/-}$ mutants

Abnormal flow makes analysis of mouse mutants challenging since it becomes a question of whether flow or loss of signaling function cause the mutant phenotype. In *n-cadherin* mutants, cardiac-specific rescue of gene expression was sufficient to rescue flow and cardiovascular defects observed in null mutants (Luo et al., 2001). As no obvious cardiac defects were detected in the *nrp-1* null mutants, we did not attempt cardiac-specific re-expression of *nrp-1*. To identify

aspects of the phenotype caused by loss of *nrp-1* function, we sought to compare embryos in the same flow environment and decided to analyze embryos in the absence of flow. We find that the geometry of the capillary plexus in *nrp-1* null embryos in a no flow environment is altered such that there are fewer branch points, longer vessel segments and larger avascular spaces between vessels, indicative of increased vessel diameter. This phenotype is seen in both no-flow and untreated *nrp-1* null embryos and therefore not related to flow. This method allowed us to identify aspects of the phenotype that are purely due to loss of Nrp-1 function. The relative simplicity of the method, as compared to transgenic rescue experiments, makes it easily applicable to analysis of numerous mouse mutants for genes involved in cardiovascular development in which abnormal flow is suspected.

## Formation of Defective Capillary Geometry in *nrp-1*$^{-/-}$ mutants

To confirm that altered yolk sac vessel geometry in *nrp-1*$^{-/-}$ mutants was due to loss of Nrp-1 function rather than to abnormal flow, we injected wild-type embryos with blocking antibodies specific to either the Sema3A or the VEGF binding domains of Nrp-1. Both antibodies decreased yolk sac vessel branching, but only the Nrp-1B VEGF blocking antibody led to phenocopy of all aspects of the *nrp1-/-* vascular morphology. Previous studies have shown that both antibodies reduce VEGF-driven endothelial cell migration and sprouting angiogenesis in various *in vitro* and *in vivo* models, with anti-Nrp-1B being slightly more potent than anti-Nrp-1A (Pan et al., 2007a). Both antibodies disrupt complex formation of Nrp-1 and VEGFR-2, suggesting that both inhibit VEGF-driven motility via disruption of complex formation and downstream signaling events. Our results agree with these findings, as inhibiting the Sema3A-binding domain showed a small effect on vascular morphology, while injection of antibodies that block the VEGF-binding domain mimicked multiple aspects of the *nrp-1*$^{-/-}$ phenotype. Furthermore, injection of antibody

blocking VEGF binding to Nrp-1 could induce the *nrp-1*$^{-/-}$ capillary phenotype in wild-type embryos experiencing normal flow. These experiments therefore clearly identify the aberrant vascular geometry as a primary defect due to loss of Nrp-1 signaling.

Endothelial replication was similar between wild-type and mutants and could not account for the altered *nrp-1*$^{-/-}$ yolk sac vessel geometry. Thus, loss of Nrp-1 function does not influence endothelial cell replication in vivo, confirming previous findings with antibodies blocking VEGF or Sema3A binding to Nrp-1, which failed to inhibit VEGF-driven endothelial proliferation in vitro (Pan et al., 2007a). We also found no differences in sprouting/regression between wild type and *nrp-1*$^{-/-}$ mutants. However, the number of PECAM positive endothelial cells extending into avascular yolk sac areas was very low (less than 1 per mm$^2$). Time-lapse studies in early quail embryos have shown that formation of the vascular plexus involves endothelial cell migration along existing endothelial cord structures as well as sprouting (Rupp et al., 2003). While sprouting appeared to be an important mechanism to generate new vascular cords, only a small fraction of endothelial cells was shown to exhibit protrusive behavior over the period of recording (Perryn et al., 2008). Thus, sprout formation in yolk sac vessels may be missed in fixed samples. We can therefore not rule out altered sprouting or regression of yolk sac endothelial cells as a potential mechanism accounting for the altered vascular morphology of *nrp-1* null yolk sacs.

We found significant differences in the pattern of endothelial migration between wild-type and *nrp-1*$^{-/-}$ mutants. Focal DiI injections showed that *nrp-1* knockout cells are found at greater distances from the injection area than wild-type cells. This observation was surprising, as one might have expected migration of *nrp-1*$^{-/-}$ cells to be decreased. However, the mutant cells appeared to migrate along existing endothelial cell cords and were never seen leaving existing vessels. Thus, rather than exhibiting a general block of migration, it appears that *nrp-1* mutant

cells fail to migrate in the proper direction, most likely via loss of VEGF signaling. Migration along existing capillaries has been shown to require cell-cell rather than extracellular matrix interactions (Rupp et al., 2003), suggesting that interactions between endothelial Nrp-1 and matrix-bound VEGF may be disrupted in the mutant mice. Loss of Nrp-1 function may thus perturb binding of extracellular matrix-bound $VEGF_{164}$, complex formation with VEGFR-2 and downstream signaling, leading to inhibition of directional migration and vessel branching, without affecting other aspects of endothelial function such as proliferation. Such a mechanism would explain the reduction in branchpoints and larger vessel diameters since the same numbers of endothelial cells are creating fewer vessels. Alternatively, as qPCR analysis has shown that *nrp-1* mutant endothelial cells express elevated *vegf* mRNA levels, increases in VEGF signaling through VEGFR-2 may cause the increase in endothelial migration we observe. We find this model unlikely, however, as *vegf* levels in cultured no-flow wild-type or *nrp-1*$^{-/-}$ mutants are similar, yet their vascular phenotypes differ. Furthermore, injection of antibodies blocking VEGF binding to Nrp-1 into wild-type embryos with normal flow and presumably unaltered VEGF levels can reproduce altered capillary geometry.

## Endothelial Gene Regulation by Nrp-1

As the maintenance of expression of arterial markers requires flow (le Noble et al., 2004), we investigated whether changes in arterial-venous gene expression in *nrp-1* mutants were created by the abnormal flow present in these embryos. We found that expression levels of arterial markers *cx40* and *efnb2* were decreased in *nrp-1* mutants compared to wild-type embryos. For *efnb2*, this change appears to be linked to extra-embryonic vessels as highlighted by the loss of expression in the vitelline artery. These two genes were previously reported downregulated in endothelial-specific conditional *Nrp-1* knockout embryos (Mukouyama et al., 2005), however the effect of flow was not analyzed. Wild-type embryos cultured in no-flow conditions showed no changes in

the expression levels of these two genes, indicating that the decrease was specific for the *nrp-1* mutation and not secondary to altered blood flow, thus confirming and extending previous reports (Mukouyama et al., 2005).

### Acknowledgements

This work was supported by grants from INSERM, Ministère de la Recherche (ANR-PCOD, ANR Neuroscience, ANR blanche), ARC (3124), Institut de France (Cino del Duca) and the European Community (LSHG-CT-2004-503573). We thank Y. Mukouyama for providing the Cx40 probe. Liz Jones was supported by the Foundation Lefoulon-Delalande and a Marie Curie Action Fellowship (IIF 022006).

## Disclosures

R. J. Watts is an employee of Genentech and the antibodies provided by him where developed by Genentech. All other authors have nothing to disclose.

# References

**Ablameyko, S. and Pridmore, T. P.** (2000). Machine Interpretation of Line Drawing Images. Secaucus, NJ: Springer-Verlag.

**Appleton, B. A., Wu, P., Maloney, J., Yin, J., Liang, W. C., Stawicki, S., Mortara, K., Bowman, K. K., Elliott, J. M., Desmarais, W. et al.** (2007). Structural studies of neuropilin/antibody complexes provide insights into semaphorin and VEGF binding. *Embo J* **26**, 4902-12.

**Beucher, S.** (1990). Segmentation d'images et morphologie mathématique. In *CMM Centre de Morphologie Mathématique*, vol. PhD Thesis (ed., pp. 294. Paris: ENSMP

**Blackman, B. R., Garcia-Cardena, G. and Gimbrone, M. A., Jr.** (2002). A new in vitro model to evaluate differential responses of endothelial cells to simulated arterial shear stress waveforms. *J Biomech Eng* **124**, 397-407.

**Chapman, W. B.** (1918). The effect of the heart-beat upon the development of the vascular system in the chick. *Am. J. Anat.* **23**, 175-203.

**Clark, E. R.** (1918). Studies on the growth of blood vessels in the tail of frog. *Am. J. Anat.* **23**, 37–88.

**Coster, M. and Chermant, J. L.** (1985). Precis d'analyse d'images. Paris: Les Editions du CNRS.

**Gagnon, M. L., Bielenberg, D. R., Gechtman, Z., Miao, H. Q., Takashima, S., Soker, S. and Klagsbrun, M.** (2000). Identification of a natural soluble neuropilin-1 that binds vascular endothelial growth factor: In vivo expression and antitumor activity. *Proc Natl Acad Sci U S A* **97**, 2573-8.

**Gerhardt, H., Ruhrberg, C., Abramsson, A., Fujisawa, H., Shima, D. and Betsholtz, C.** (2004). Neuropilin-1 is required for endothelial tip cell guidance in the developing central nervous system. *Dev Dyn* **231**, 503-9.

**Grazioli, A., Alves, C. S., Konstantopoulos, K. and Yang, J. T.** (2006). Defective blood vessel development and pericyte/pvSMC distribution in alpha 4 integrin-deficient mouse embryos. *Dev Biol* **293**, 165-77.

**Gu, C., Rodriguez, E. R., Reimert, D. V., Shu, T., Fritzsch, B., Richards, L. J., Kolodkin, A. L. and Ginty, D. D.** (2003). Neuropilin-1 conveys semaphorin and VEGF signaling during neural and cardiovascular development. *Dev Cell* **5**, 45-57.

**He, Z. and Tessier-Lavigne, M.** (1997). Neuropilin is a receptor for the axonal chemorepellent Semaphorin III. *Cell* **90**, 739-51.

**Jones, E. A., Baron, M. H., Fraser, S. E. and Dickinson, M. E.** (2004). Measuring hemodynamic changes during mammalian development. *Am J Physiol Heart Circ Physiol* **287**, H1561-9.

**Jones, E. A., Crotty, D., Kulesa, P. M., Waters, C. W., Baron, M. H., Fraser, S. E. and Dickinson, M. E.** (2002). Dynamic in vivo imaging of postimplantation mammalian embryos using whole embryo culture. *Genesis* **34**, 228-35.

**Kawasaki, T., Kitsukawa, T., Bekku, Y., Matsuda, Y., Sanbo, M., Yagi, T. and Fujisawa, H.** (1999). A requirement for neuropilin-1 in embryonic vessel formation. *Development* **126**, 4895-902.

**Kitsukawa, T., Shimizu, M., Sanbo, M., Hirata, T., Taniguchi, M., Bekku, Y., Yagi, T. and Fujisawa, H.** (1997). Neuropilin-semaphorin III/D-mediated

chemorepulsive signals play a crucial role in peripheral nerve projection in mice. *Neuron* **19**, 995-1005.

**Kolodkin, A. L., Levengood, D. V., Rowe, E. G., Tai, Y. T., Giger, R. J. and Ginty, D. D.** (1997). Neuropilin is a semaphorin III receptor. *Cell* **90**, 753-62.

**le Noble, F., Moyon, D., Pardanaud, L., Yuan, L., Djonov, V., Matthijsen, R., Breant, C., Fleury, V. and Eichmann, A.** (2004). Flow regulates arterial-venous differentiation in the chick embryo yolk sac. *Development* **131**, 361-75.

**Lucitti, J. L., Jones, E. A., Huang, C., Chen, J., Fraser, S. E. and Dickinson, M. E.** (2007). Vascular remodeling of the mouse yolk sac requires hemodynamic force. *Development* **134**, 3317-26.

**Luo, Y., Ferreira-Cornwell, M., Baldwin, H., Kostetskii, I., Lenox, J., Lieberman, M. and Radice, G.** (2001). Rescuing the N-cadherin knockout by cardiac-specific expression of N- or E-cadherin. *Development* **128**, 459-69.

**May, S. R., Stewart, N. J., Chang, W. and Peterson, A. S.** (2004). A Titin mutation defines roles for circulation in endothelial morphogenesis. *Dev Biol* **270**, 31-46.

**Meeson, A., Palmer, M., Calfon, M. and Lang, R.** (1996). A relationship between apoptosis and flow during programmed capillary regression is revealed by vital analysis. *Development* **122**, 3929-38.

**Miao, H. Q., Soker, S., Feiner, L., Alonso, J. L., Raper, J. A. and Klagsbrun, M.** (1999). Neuropilin-1 mediates collapsin-1/semaphorin III inhibition of endothelial cell motility: functional competition of collapsin-1 and vascular endothelial growth factor-165. *J Cell Biol* **146**, 233-42.

**Moyon, D., Pardanaud, L., Yuan, L., Breant, C. and Eichmann, A.** (2001a). Plasticity of endothelial cells during arterial-venous differentiation in the avian embryo. *Development* **128**, 3359-70.

**Moyon, D., Pardanaud, L., Yuan, L., Breant, C. and Eichmann, A.** (2001b). Selective expression of angiopoietin 1 and 2 in mesenchymal cells surrounding veins and arteries of the avian embryo. *Mech Dev* **106**, 133-6.

**Mukouyama, Y. S., Gerber, H. P., Ferrara, N., Gu, C. and Anderson, D. J.** (2005). Peripheral nerve-derived VEGF promotes arterial differentiation via neuropilin 1-mediated positive feedback. *Development* **132**, 941-52.

**Pan, Q., Chanthery, Y., Liang, W. C., Stawicki, S., Mak, J., Rathore, N., Tong, R. K., Kowalski, J., Yee, S. F., Pacheco, G. et al.** (2007a). Blocking neuropilin-1 function has an additive effect with anti-VEGF to inhibit tumor growth. *Cancer Cell* **11**, 53-67.

**Pan, Q., Chanthery, Y., Wu, Y., Rahtore, N., Tong, R. K., Peale, F., Bagri, A., Tessier-Lavigne, M., Koch, A. W. and Watts, R. J.** (2007b). Neuropilin-1 binds to VEGF121 and regulates endothelial cell migration and sprouting. *J Biol Chem*.

**Perryn, E. D., Czirok, A. and Little, C. D.** (2008). Vascular sprout formation entails tissue deformations and VE-cadherin-dependent cell-autonomous motility. *Dev Biol* **313**, 545-55.

**Ruhrberg, C., Gerhardt, H., Golding, M., Watson, R., Ioannidou, S., Fujisawa, H., Betsholtz, C. and Shima, D. T.** (2002). Spatially restricted patterning cues provided by heparin-binding VEGF-A control blood vessel branching morphogenesis. *Genes Dev* **16**, 2684-98.

**Rupp, P. A., Czirok, A. and Little, C. D.** (2003). Novel approaches for the study of vascular assembly and morphogenesis in avian embryos. *Trends Cardiovasc Med* **13**, 283-8.

**Serini, G., Valdembri, D., Zanivan, S., Morterra, G., Burkhardt, C., Caccavari, F., Zammataro, L., Primo, L., Tamagnone, L., Logan, M. et al.** (2003). Class 3 semaphorins control vascular morphogenesis by inhibiting integrin function. *Nature* **424**, 391-7.

**Shraga-Heled, N., Kessler, O., Prahst, C., Kroll, J., Augustin, H. and Neufeld, G.** (2007). Neuropilin-1 and neuropilin-2 enhance VEGF121 stimulated signal transduction by the VEGFR-2 receptor. *Faseb J* **21**, 915-26.

**Soker, S., Takashima, S., Miao, H. Q., Neufeld, G. and Klagsbrun, M.** (1998). Neuropilin-1 is expressed by endothelial and tumor cells as an isoform-specific receptor for vascular endothelial growth factor. *Cell* **92**, 735-45.

**Suchting, S., Freitas, C., le Noble, F., Benedito, R., Breant, C., Duarte, A. and Eichmann, A.** (2007). The Notch ligand Delta-like 4 negatively regulates endothelial tip cell formation and vessel branching. *Proc Natl Acad Sci U S A* **104**, 3225-30.

**Thoma, R.** (1893). Untersuchungen über die Histogenese und Histomechanikdes Gefässsytems. Stuttgart: Ferdinand Enke.

**Vieira, J. M., Schwarz, Q. and Ruhrberg, C.** (2007). Selective requirements for NRP-1 ligands during neurovascular patterning. *Development* **134**, 1833-43.

**Wakimoto, K., Kobayashi, K., Kuro, O. M., Yao, A., Iwamoto, T., Yanaka, N., Kita, S., Nishida, A., Azuma, S., Toyoda, Y. et al.** (2000). Targeted disruption

of Na+/Ca2+ exchanger gene leads to cardiomyocyte apoptosis and defects in heartbeat. *J Biol Chem* **275**, 36991-8.

**You, L. R., Lin, F. J., Lee, C. T., DeMayo, F. J., Tsai, M. J. and Tsai, S. Y.** (2005). Suppression of Notch signalling by the COUP-TFII transcription factor regulates vein identity. *Nature* **435**, 98-104.

**Yuan, L., Moyon, D., Pardanaud, L., Breant, C., Karkkainen, M. J., Alitalo, K. and Eichmann, A.** (2002). Abnormal lymphatic vessel development in neuropilin 2 mutant mice. *Development* **129**, 4797-806.

# Figure Legends

**Figure 1 – Cardiovascular Phenotype of *nrp-1*$^{-/-}$ Embryos.** Dark field images of freshly dissected yolk sacs from E9.5 embryos with the indicated genotypes (A, E) shows defects in yolk sac vascular remodeling that are further highlighted by PECAM-1 staining of the wild-type (B) and mutant (F) yolk sacs. Angiograms at E8.5, just after the onset of plasma flow, (C, G) show that vessels are lumenized in both wild-type (C) and knockout (G) embryos, but that *Nrp-1*$^{-/-}$ already show altered yolk sac vessel geometry (G). PECAM-1 stainings of yolk sacs (D,H) were used to quantitate the phenotype based on the number of branchpoints per mm$^2$ (I), average vessel segment length (J) and area of avascular spaces (K) at different stages of development for wild-type and knockout embryos. * $p<0.05$, ** $p<0.01$, *** $p<0.005$ student's two tailed t-test. Scale bars; 1mm (A, E), 500 μm (B, C, F, G) 100 μm (D, H).

**Figure 2 – Investigating Causes of Defective Flow in Nrp-1$^{-/-}$ Embryos.** In situ hybridization with a *nrp-1* antisense riboprobe on a section from a wild-type embryo at 10 somites (A) shows expression in the atrium (marked A) and not the ventricle (marked V), as well as expression in the dorsal aortae (arrows) and yolk sac vessels (arrowheads). Serial sections of E8.5 wild-type (B) and mutant (D) embryos stained for PECAM-1 show that dorsal aortae (marked DA) are present and lumenized in both cases, though often collapsed in the mutant (D). By E9.5, Collagen IV staining highlights the dorsal aortae (DA), gut (G) and heart (H) of wild-type embryos (C). In mutant embryos, one or both dorsal aortae are often missing (E, arrow). Intersomitic vessel sprouting is visible in E9.5 wild-type embryos stained for PECAM-1 (F) but is delayed in mutant embryos (G) and also shows the collapsed dorsal aorta (arrow). The cephalic region of E9.5 wild-type embryos shows an extensive vasculature (H) that is also present in the mutant embryos

(I), however the vasculature of the mutants is more sparse and many vessels do not appear to be lumenized. The internal carotid artery (ICA) has started forming in the wild-type (H) but is lacking in the mutant (I). Scale bars; 50 μm (A, B, D), 100 μm (F, G, H, I), 200 μm (C, E).

**Figure 3 – Separating the Role of Blood Flow from *Nrp-1* Function.** PECAM-1 staining of yolk sacs from cultured heterozygote and mutant embryos in both flow and no-flow conditions, as indicated (A). In heterozygote embryos with flow, a large remodeled artery (Art) is visible. Heterozygote embryos without flow fail to remodel capillaries into large vessels. *Nrp-1*$^{-/-}$ vessels, with or without flow, show decreased branching (B), increased vessel segment length (C) and increased avascular spaces (D). Inlays in (A) show collagen IV staining on sections from E9.5 yolk sacs that also highlight the large vessel diameters in *nrp-1*$^{-/-}$ yolk sacs compared to wild-type. ** $p<0.01$, *** $p<0.005$ student's two tailed t-test. Scale bars; 100 μm.

**Figure 4 – Blocking Nrp-1 Function Reproduces the *nrp-1*-/- Yolk Sac Vessel Phenotype.** Wild-type embryos from a CD-1 background were treated with various proteins by intracardiac injection followed by whole embryo culture. Subsequent to culture, the vasculature was fixed and stained for PECAM-1 (A-D). The images were quantified for vascular morphology (E-G). Untreated embryos showed remodeling, typical of E9.5 embryos (A). $VEGF_{120}$ injection caused an increase in overall vascular coverage (B). Injection of antibodies against Nrp-1, which are reported to block Sema3A binding (C) and VEGF binding (D) to Nrp-1 respectively (Pan et al., 2007b), were both effective at decreasing the number of branchpoints and increasing vessel segment length as seen in the *Nrp-1*$^{-/-}$ embryos (E, F). Injection of both antibodies did not show a synergistic effect on the number of branchpoints. Only antibodies against the VEGF binding domain of Nrp-1 were capable of increasing average area of avascular space, as seen in *Nrp-1*$^{-/-}$ embryos (G). Injection of Sem3A and sNrp-1 had no statistically significant effect on capillary

geometry (E-G). * p<0.05, ** p<0.01, *** p<0.005, student two-tailed t-test. Scale bars; 100 μm.

**Figure 5 – Replication, Sprouting and Migration in *nrp-1*$^{-/-}$ yolk sacs.** Endothelial replication was quantitated using double staining with phospho-histone 3 and PECAM-1 at different stages of development (A). No statistically significant difference was seen at any of the stages examined. The number of PECAM-1 positive unconnected segments extending into avascular spaces, which may represent sprouts or regressing vessels, was assessed from images of the yolk sac at E9.5 (B). No significant differences were observed between the different groups. Endothelial cell migration was assessed by focal injection of cell tracker CM-DiI into a capillary region (C-G) of the yolk sac followed by quantification of the maximum migration distance per embryo (C). The initial injection site can be observed in the white light images (red arrows, D & E). Endothelial cells did not migrate very far away from the site of injection in wild-type embryos (F) but were seen migrating longer distances along existing capillaries for knockout embryos (G). * p<0.05, student's two tailed t-test. Scale bar; 1mm.

**Figure 6 – Arterial Venous Gene Expression in *nrp-1*$^{-/-}$ Embryos.** A-F: Serial sections were stained by in situ hybridization for *dll4* (A, B), *cx40* (C, D), *efnb2* (E, F) in both wild-type (A, C, E) and *nrp-1* knockout embryos (B, D, F) at 20 somites. Images show the common atrial chamber (CAC), the vitelline artery (VA) and the dorsal aortae (DA) at either the level of the heart (A-D) or at the caudal end of the embryo (E, F). B: Red arrow denotes a missing dorsal aorta in the *nrp-1*$^{-/-}$ embryo, note that the remaining dorsal aorta still expresses *dll4*. D: Note absence of *cx40* expression in *nrp-1*$^{-/-}$ embryos. F: Normal expression of *efbn2* is present in dorsal aorta and somites of *nrp-1*$^{-/-}$ embryos, but lacking in the vitelline artery. G: Levels of gene expression were measured from isolated endothelial cells, either pooled wild-type/heterozygous

(denoted wild-type) or knockout, both with and without blood flow for 11 cardiovascular genes; 4 pan-endothelial genes, 4 arterial genes and 3 venous genes. Gene expression was normalized to three housekeeping genes; *α-tubulin, β-actin and gapdh*. Note that expression of *cx40* and *efbn2* in *nrp-1*$^{-/-}$ is downregulated compared to wild-type regardless of flow environment. * $p<0.05$, **$p<0.01$, ***$p<0.005$, student's two-tailed t-test. Scale bars; 100 μm.

# Supplementary Figure Legend

**Figure 1 – Illustration of morphometry used for quantifying vessel geometry in wild-type and *nrp-1* homozygous mutant yolk sacs.** PECAM-1 stainings of wild-type (A) and knockout (C) yolk sacs were used to quantitate the vascular phenotype. Images were first thresholded to create binary images (B,D). Total vessel area was assessed by counting the number of red vs black pixels in the binary images. A vessel skeleton (blue lines) was extracted from the binary images using computer software (see Methods). Points where the skeleton lines intersect (white dots) are counted as branchpoints. Segment length was assessed by dividing the total length of all skeleton lines by the number of intersections. If the total vessel area is constant, and the number of vessel branchpoints is reduced, one expects that the length of individual vessel segments increases. Vessel diameter was assessed indirectly, by measuring the average area of an avascular space (hole) between vessels. With constant vessel area and increased space between vessels, it follows that the individual segments must be thicker. Scale bar; 100 μm.

# Tables

Table I – Blood Flow in Neuropilin Mutant Embryos

| Embryonic Stage | *nrp1*$^{+/+}$ *or nrp1*$^{+/-}$ | *nrp-1*$^{-/-}$ |
|---|---|---|
| E8.5 (10 somites) Continuous Circulation | 100% Continuous Circulation (n=12) | 14% Continuous Circulation<br>86% Oscillatory Circulation (n=7) |
| E9.5 of Circulation | 100% Normal Circulation (n=13) | 100% Absence (n=4) |

Figure 1

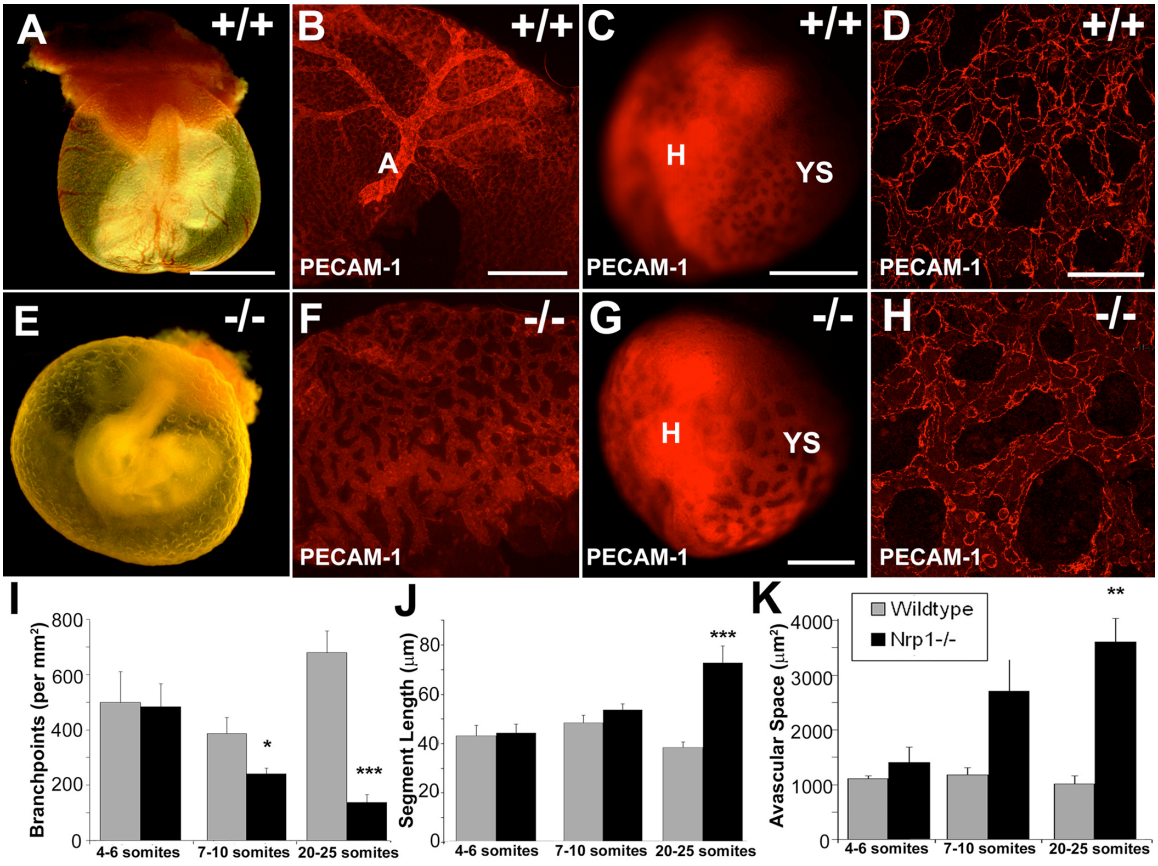
A
+/+
B
+/+
A
PECAM-1
C
+/+
H
YS
PECAM-1
D
+/+
PECAM-1
E
-/-
F
-/-
PECAM-1
G
-/-
H
YS
PECAM-1
H
-/-
PECAM-1
I
Branchpoints (per mm²)
800
600
400
200
0
*
***
4-6 somites
7-10 somites
20-25 somites
J
Segment Length (μm)
80
60
40
20
0
***
4-6 somites
7-10 somites
20-25 somites
K
Avascular Space (μm²)
4000
3000
2000
1000
0
Wildtype
Nrp1-/-
**
4-6 somites
7-10 somites
20-25 somites

Figure 2

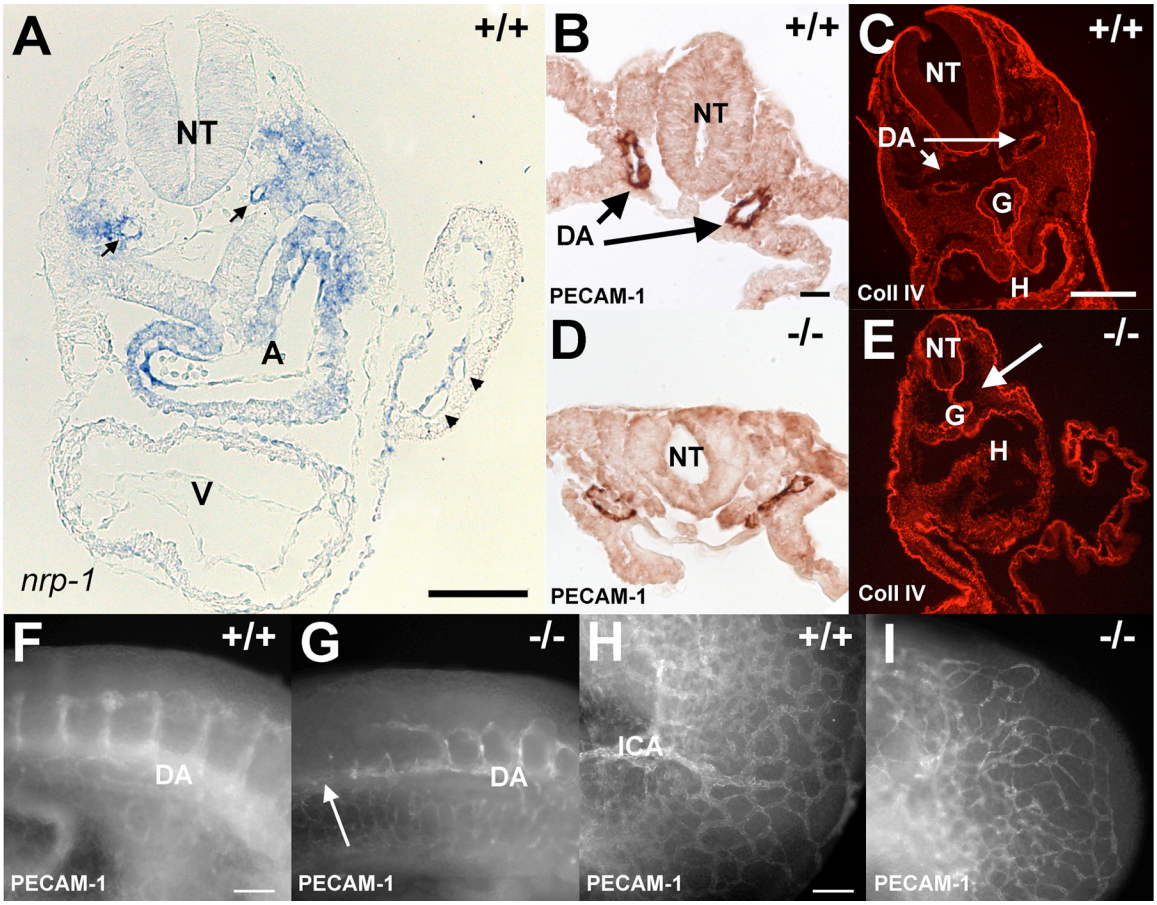
A
+/+
NT
A
V
nrp-1
B
+/+
NT
DA
PECAM-1
C
+/+
NT
DA
G
Coll IV
H
D
-/-
NT
PECAM-1
E
-/-
NT
G
H
Coll IV
F
+/+
DA
PECAM-1
G
-/-
DA
PECAM-1
H
+/+
ICA
PECAM-1
I
-/-
PECAM-1

Figure 3

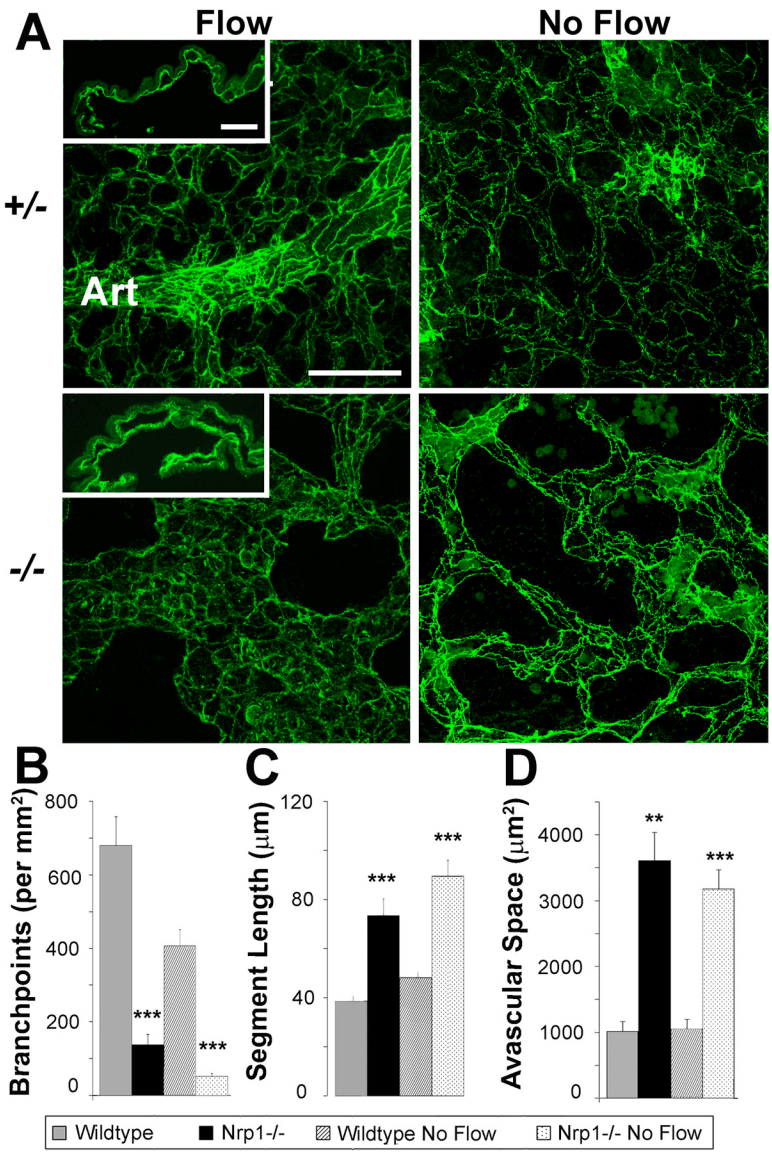
A
Flow
No Flow
+/-
-/-
Art
B
Branchpoints (per mm²)
800
600
400
200
0
***
***
C
Segment Length (μm)
120
80
40
0
***
***
D
Avascular Space (μm²)
4000
3000
2000
1000
0
**
***
Wildtype
Nrp1-/-
Wildtype No Flow
Nrp1-/- No Flow

Figure 4

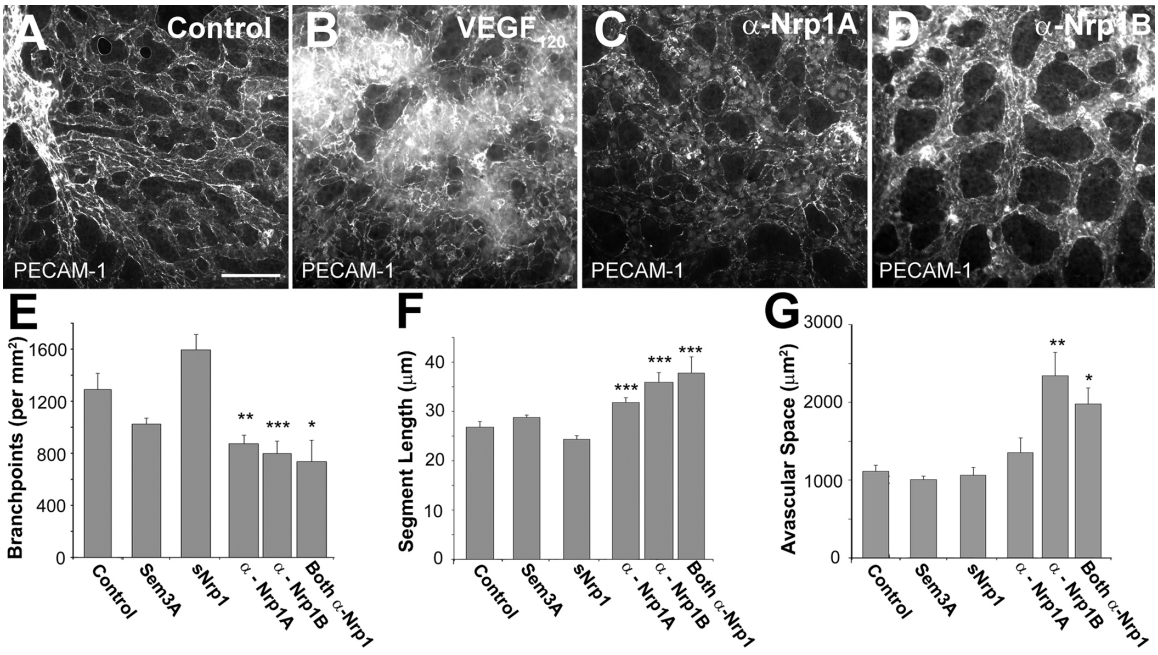
A
Control
PECAM-1
B
VEGF120
PECAM-1
C
α-Nrp1A
PECAM-1
D
α-Nrp1B
PECAM-1
E
Branchpoints (per mm²)
0
400
800
1200
1600
**
***
*
Control
Sem3A
sNrp1
α - Nrp1A
α - Nrp1B
Both α-Nrp1
F
Segment Length (μm)
0
10
20
30
40
***
***
***
Control
Sem3A
sNrp1
α - Nrp1A
α - Nrp1B
Both α-Nrp1
G
Avascular Space (μm²)
0
1000
2000
3000
**
*
Control
Sem3A
sNrp1
α - Nrp1A
α - Nrp1B
Both α-Nrp1

Figure 5

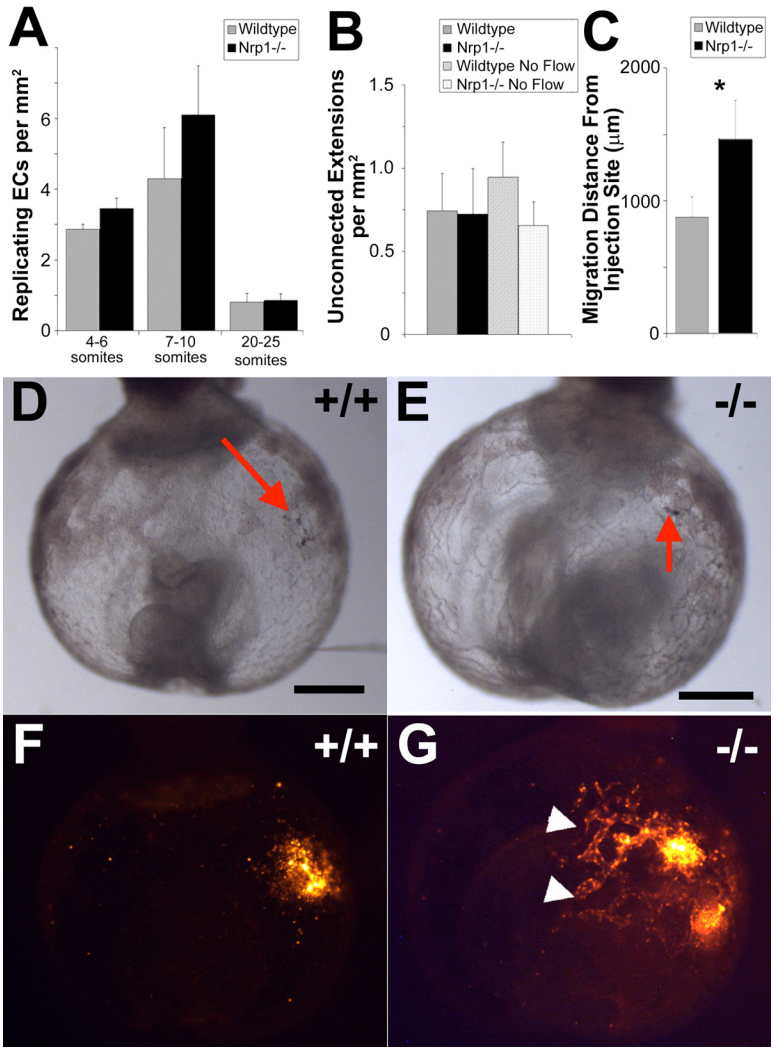
A
Wildtype
Nrp1-/-
Replicating ECs per mm²
0
2
4
6
4-6 somites
7-10 somites
20-25 somites
B
Wildtype
Nrp1-/-
Wildtype No Flow
Nrp1-/- No Flow
Unconnected Extensions per mm²
0
0.5
1.0
1.5
C
Wildtype
Nrp1-/-
Migration Distance From Injection Site (μm)
0
1000
2000
*
D
+/+
E
-/-
F
+/+
G
-/-

Figure 6

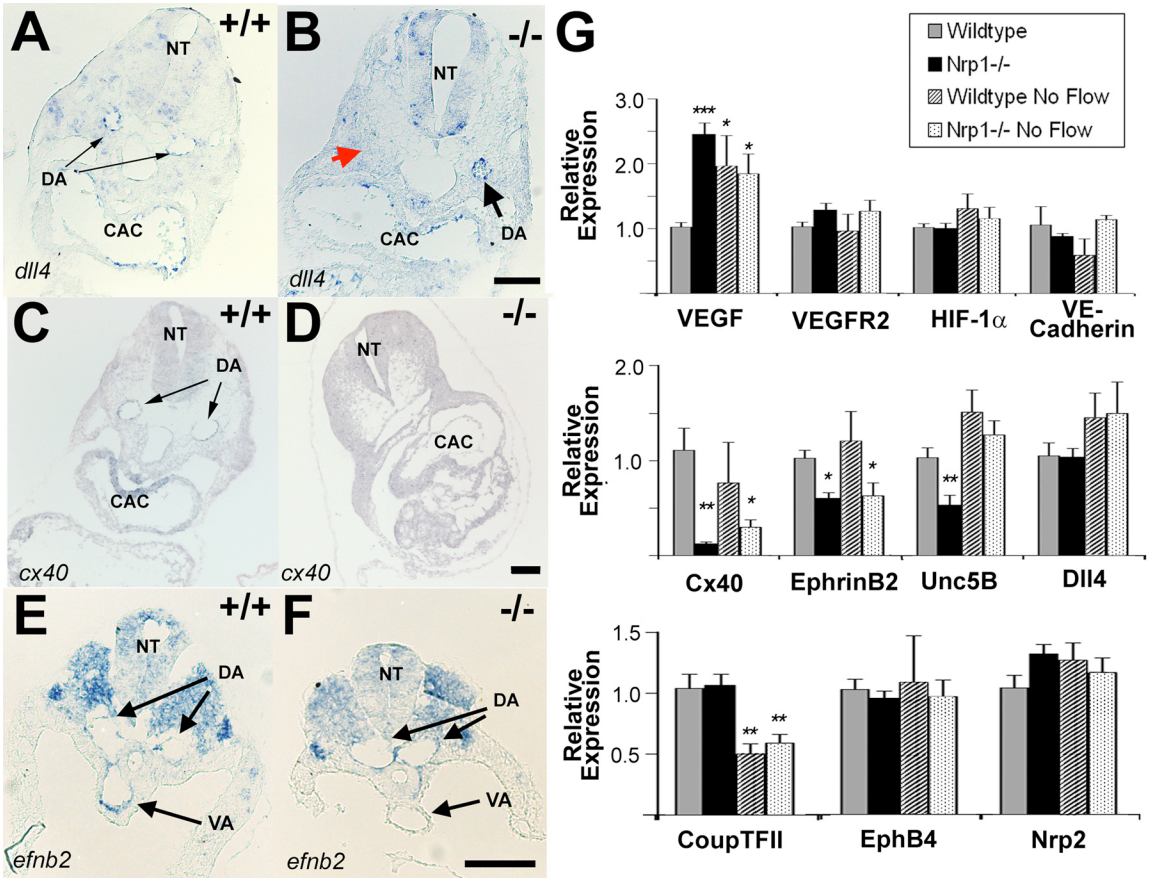
A
+/+
NT
DA
CAC
dll4
B
-/-
NT
CAC
DA
dll4
C
+/+
NT
DA
CAC
cx40
D
-/-
NT
CAC
cx40
E
+/+
NT
DA
VA
efnb2
F
-/-
NT
DA
VA
efnb2
G
Wildtype
Nrp1-/-
Wildtype No Flow
Nrp1-/- No Flow
Relative Expression
3.0
2.0
1.0
VEGF
VEGFR2
HIF-1α
VE-Cadherin
2.0
1.0
Cx40
EphrinB2
Unc5B
Dll4
1.5
1.0
0.5
CoupTFII
EphB4
Nrp2

Supplementary Figure 1